O_2 and Vacancy Diffusion on Rutile(110): Pathways and Electronic Properties

Antonio Tilocca and Annabella Selloni*[a]

The binding structures and diffusion pathways of molecular oxygen on a defective TiO_2(110) surface are studied by means of a recently developed first-principles string molecular dynamics approach. A variety of molecular and dissociated O_2 adsorption states are identified and the kinetics of their interconversion is analyzed. These results, as well as calculations of the electronic properties and of scanning tunneling microscopy (STM) images, are used to discuss recent experimental observations of the interactions between surface oxygen vacancies and the adsorbed oxygen molecule.

Introduction

Titanium dioxide (TiO_2) surfaces are involved in a wide variety of applications, ranging from photocatalysis to gas sensors and biomaterials.[1–3] The interaction of the surface with O_2 plays an important role in these applications; for instance, a well-established role of adsorbed oxygen is to scavenge photoexcited electrons from the TiO_2 conduction band[6] thus preventing electron–hole recombination. Similarly, when O_2 is adsorbed on a defective TiO_2 surface, it removes electrons trapped at the surface O-vacancies, forming an anionic O_2 species.[4,7] For this reason, investigation of oxygen adsorption at vacancies may be useful to understand better electron-scavenging effects in photocatalysis.[6]

Time-resolved STM measurements on the rutile TiO_2(110) surface have recently provided evidence of a strong interaction between molecular oxygen and surface vacancies.[8,9] Most noticeably, it was shown that vacancy–O_2 interactions are essential for the vacancy migration process: vacancies were observed to diffuse perpendicularly to the bridging oxygen atom rows, and this process occurred only in the presence of a "mediating" O_2 molecule. A sequence of diffusive and dissociative steps was proposed to explain these observations,[8] but subsequent total-energy DFT calculations suggested that such a vacancy-migration mechanism involved very high energy barriers.[11] Thus, an alternative mechanism was proposed, which did not involve the energetically unfavorable abstraction of a surface-bridging oxygen.[11] In this paper we reconsider the problem of oxygen–vacancy interaction on TiO_2(110): our purpose is to provide an accurate description of the pathways and barriers for all the relevant steps in the vacancy migration process, by using a recently implemented method to find minimum-energy paths in the framework of the Car–Parrinello molecular dynamics approach.[12,13] The character of the adsorbed oxygen on the defective TiO_2 surface and the surface-to-molecule charge transfer are discussed, and STM images of all the relevant stable states are presented and compared to experiment.

Results and Discussion

O_2 Adsorption Structures and Energies

The energies of the most stable oxygen adsorption states are reported in Table 1. To check cell and size effects, three different surface supercells have been used (see Figure 1). The optimized structures are shown in Figure 2, and they include four molecular and two dissociated states (only the most-stable dissociated state, O1, is included in Fig. 2). The geometries of the

Table 1. Energies of relevant O_2 adsorption structures (see Figure 2) optimized using different supercells on the defective rutile(110) surface. Energies [eV] are relative to V1.

	$c(2\times4)$	$p(1\times3)$	$p(2\times2)$
V1	0	0	0
V2	0.39	0.04	0.70
V5	0.91	0.65	2.01
V6	0.86	0.70	1.87
O1	0.15	−0.27	0.30
O2	1.07	0.92	1.47

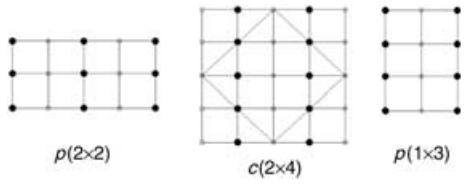

Figure 1. Schematic top view of the surface cells examined herein. Full and empty circles represent bridging oxygen and five-fold-coordinated Ti atoms, respectively.

[a] *Dr. A. Tilocca, Prof. A. Selloni*
Department of Chemistry, Princeton University
Princeton, NJ 08544 (USA)
Fax:(+1) 609-258-6746

 DOI: 10.1002/cphc.200400570

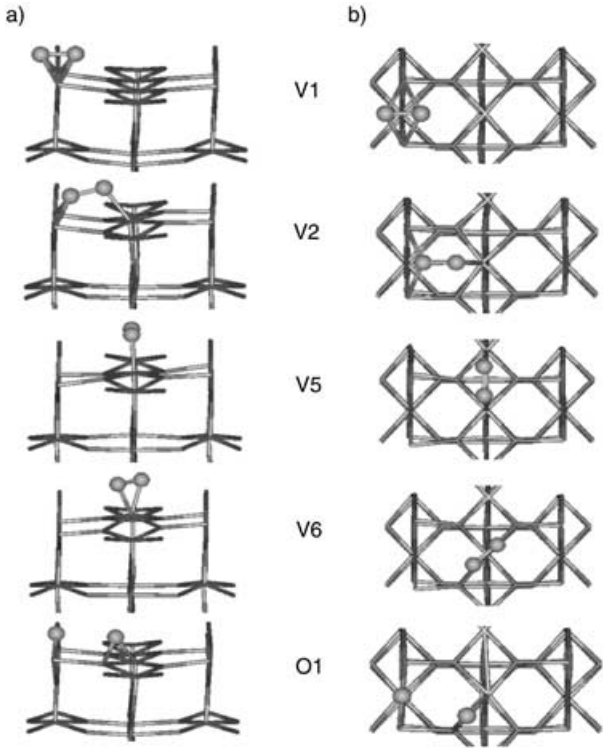

Figure 2. Optimized oxygen adsorption structures obtained using the $c(2\times4)$ cell: a) side view, b) top view. Ti and O atoms of the slab are represented as dark and light gray sticks, respectively, while adsorbed O atoms are represented as large spheres.

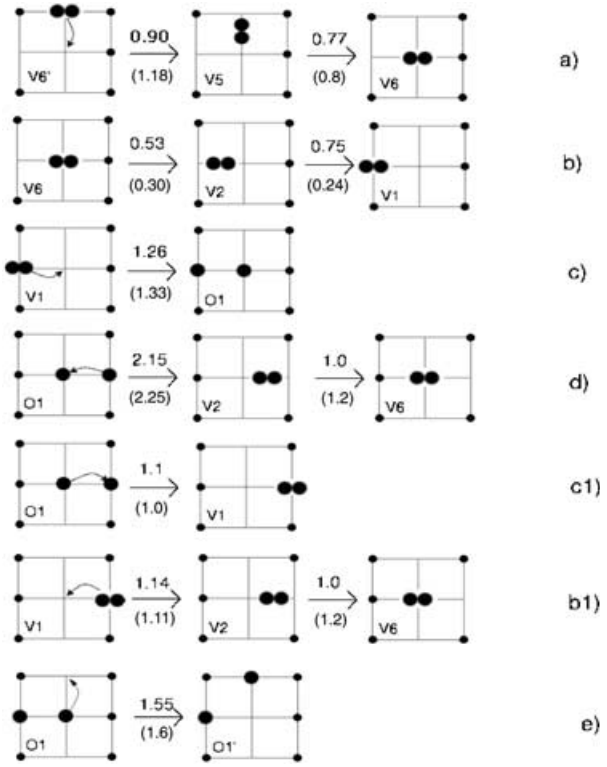

Figure 3. Schematic representation of the vacancy migration mechanisms. The calculated potential-energy barriers for $c(2\times4)$ and $p(2\times2)$ cells (in parentheses) are also reported. Small and large black dots represent lattice and adsorbed oxygen, respectively.

molecular states are similar to those reported in other recent first-principles calculations.[14,15] In V1, the O_2 molecule fills the vacancy with its bond axis perpendicular to the oxygen row; in V6 it is adsorbed on a fivefold-coordinated Ti site (Ti_{5c}) adjacent to the vacancy. Between these two states, a stable V2 minimum is found, in which the molecule is located halfway between the vacancy and the Ti_{5c}. Along the row of Ti_{5c} sites another stable intermediate, V5, is present with the O–O axis parallel to the row. Upon dissociation, one O atom fills the vacancy and the other is adsorbed on a Ti_{5c} atom. In the most-stable dissociated state O1, the O–Ti5c axis is not perpendicular to the surface plane, as in refs. [14] and [15], but is bent by 42°. In our calculations, structure O2, where the O adatom binds exactly on top of Ti_{5c}, is much less stable. The relative stability decreases in the order V1, V2, V6, V5 for the molecular adsorption. The same ordering was found in the three different cells, although relative energies are considerably larger for the $p(2\times2)$ cell. A stronger dependence on the choice of the surface supercell is found for the relative stability of the V1 and O1 structures, for example, O1 is the most stable state in the $p(1\times3)$ cell.

Oxygen Diffusion Pathways

The minimum energy pathways (MEPs) for several elementary diffusive and dissociative steps involving the stable states described above were determined, see Figure 3. These include: a) molecular diffusion along the row of Ti_{5c} sites (V6→V6′); b) diffusion of the molecule from the vacancy to the adjacent Ti_{5c} along $[1\bar{1}0]$ (V6→V1); c) dissociation of the molecule in the vacancy, leading to a "perfect" surface plus an oxygen adatom (V1→O1); d) capture of a bridging oxygen by the O adatom (O1→V6); e) adatom diffusion along the Ti_{5c} row (O1→O1′). In (a) and (e), V6′ and O1′ represent final states for the diffusion along the Ti_{5c} row. The potential-energy barriers for these processes have been obtained from the corresponding potential energy profiles along the MEPs. These were calculated using the $c(2\times4)$ and $p(2\times2)$ surface cells, as shown in Figure 4.

The mechanism of vacancy migration proposed in ref. [8] proceeds through steps a), b) and c). The in-row migration (a) of an adsorbed O_2 molecule and its subsequent jump (b) to a neighboring vacancy display relatively low barriers, between 0.5 and 0.8 eV in the $c(2\times4)$ cell. Both processes involve a stable intermediate. In the diffusion along the row of Ti_{5c} sites the molecule rotates along its C_2 axis, forming the V5 intermediate where it is bridging between the two Ti_{5c} atoms, with the O–O axis parallel to the Ti row; a further rotation then leads to the final state (V6). From here, molecular diffusion into a vacancy (b) involves another stable intermediate, V2, where one O atom is still bonded to the initial Ti_{5c} and the other is coordinated to both unsaturated Ti atoms on the vacancy. The next step (c) is the dissociation of the V1 state: V1→O1 (c). At variance with the MEP obtained in refs. [14] and [15], we did not find any intermediate in this process. This could be related to the different final state: in our case we considered the more

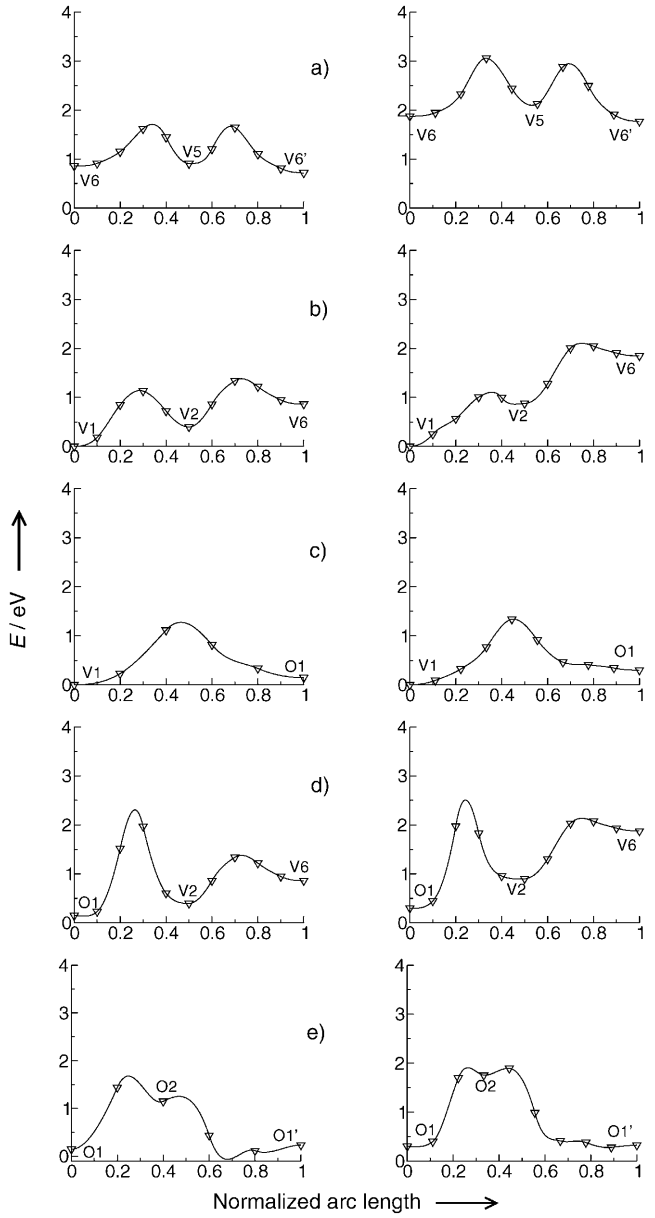

Figure 4. Potential-energy profiles along the minimum energy paths for (a)–(e) transitions: a) $c(2\times4)$ cell, b) $p(2\times2)$ cell. A cubic polynomial was used for interpolation between adjacent replicas.

stable O1 state as dissociation product, while O2 was the final state in refs. [14] and [15].

When we turn to the next step of the vacancy-migration process, according to the model of ref. [8] the O adatom captures a bridging oxygen thus forming a new vacancy, shifted by one lattice constant across the parallel rows. This process, d), again involves the V2 intermediate, whose formation from O1 shows a rather high barrier, greater than 2 eV. It could be argued that if the initial state was the less-stable O2 instead of O1, a lower barrier could probably result;[15] however our MEP for the O1→V2 process does not show any evidence of a possible O2 intermediate located between the two states (a very shallow O2 minimum is observed only along the O1→O1′ path, Figure 4e). In view of the high energy barriers involved in the vacancy diffusion model of ref. [8], a more favorable, indirect path describing the formation of a new vacancy starting from O1 was suggested in ref. [11]. The latter pathway proceeds through steps c1) and b1) in Figure 3, which are the reverse of c) and b): the O adatom moves to the vacancy forming another V1 structure, which then diffuses out of the vacancy. The energy barriers estimated through the string-method optimizations for these processes (Figure 4) are about 1.1 eV, thus confirming the more favorable kinetics for this indirect process.

Experimentally, the temperature dependence of O_2 adsorption has been studied by means of temperature programmed desorption (TPD), energy loss spectroscopy (ELS), and isotopic labeling.[7,10] At adsorption temperatures below 150 K, both molecular (on Ti_{5c} sites) and dissociative channels are observed, while dissociative adsorption is dominant above 150 K. The O_2–Ti_{5c} molecules desorb at 410 K, while O–Ti_{5c} adatoms formed by dissociation desorb above 600 K.[10] The dissociation of an O_2 molecule initially adsorbed far from a vacancy may involve several jumps along the Ti_{5c} row until a Ti_{5c} site adjacent to a vacancy is found, followed by migration into the vacancy and dissociation. These steps, labeled a)–c) in Figure 3, involve energy barriers between 0.7 and 1.3 eV: thus it is expected that not all adsorbed oxygen molecules are dissociated at low temperature. Starting from a surface where both O1 and V6 adsorption states coexist, the difference between the calculated binding energies of V6 (1.8 eV) and of an O adatom (2.33 eV[18]) is consistent with the 200 K difference between their desorption temperatures. The calculated barrier for the migration of O adatoms along the Ti_{5c} row is rather large, 1.55 eV (step e) in Figure 3). Such a large barrier may prevent each O_2 molecule from filling more than one vacancy, in agreement with the experimental observation[7] of 1:1 ratio between vacancies and adsorbed O_2 at adsorption temperatures above 150 K.

Electronic Properties

It is well established that charge transfer from vacancy-related states plays a key role in stabilizing O_2 on rutile(110): adsorption does not occur on the defect-free surface.[2,7,11,14] However, further studies are needed to understand the exact nature both of active oxygen intermediates formed in photocatalytic processes,[3,4,6] and of adsorbed O_2 species near surface defects.[7,10]

Information on the charge transfer from the vacancy to the adsorbed oxygen can be obtained from the density of states (DOS) calculated for the stable states discussed above. The bottom panel in Figure 5 shows the total DOS for the perfect slab aligned with the DOS of an isolated oxygen molecule. The O_2 LUMO (π^* orbitals) lies at the bottom of the slab conduction band, at the same energy where the oxygen vacancy state is predicted to occur by our calculations.[20] This overlap favors charge transfer from the vacancy to the O_2 molecule. In states V1 and O1, the molecular π^* orbitals are completely filled, and well below the valence band maximum, so that the gap is identical to that for the clean surface. This indicates a large

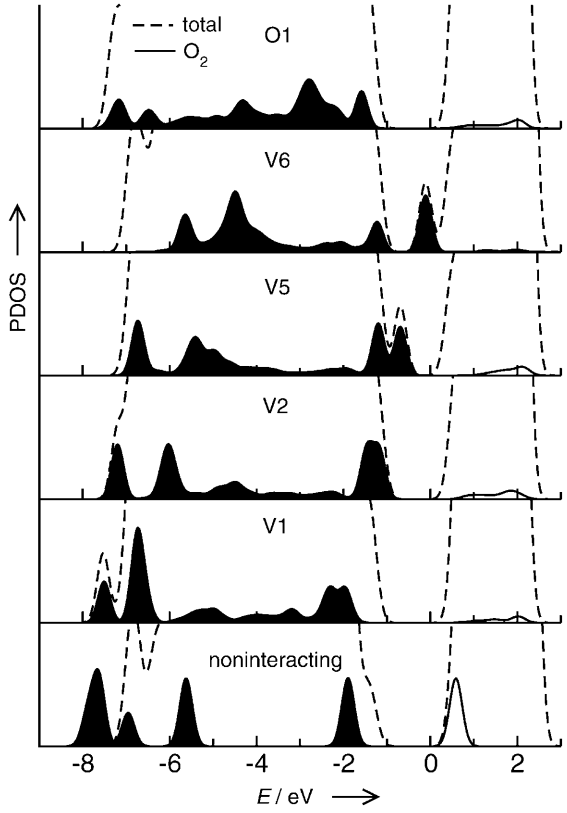

Figure 5. Calculated electronic densities of states: total (-----) and projected on O_2 (—— for filled and hollow for unoccupied states) densities of states for isolated and interacting oxygen adsorption structures. The zero of energy corresponds to the conduction band minimum.

charge transfer to the O_2 molecule: indeed the O–O bond length for V1 is expanded by 0.2 Å compared to the gas-phase value, as in an O_2^{2-} ion. When the molecule diffuses out of the vacancy, the O_2 π^* energy is raised and the gap decreases gradually in the order V1, V2, V5, V6. This could be interpreted as an indication that some charge is transferred back to the vacancy state. However the O–O distance only shows a small decrease going from V1 (1.45 Å) to V5 (1.40 Å), and for V6 and V6′ states its value actually matches V1. The calculated Löwdin partial charges on the O_2 atoms in the different adsorption states are also very similar. In other words, there is evidence of a significant vacancy→O_2 charge transfer for all the adsorption states, in which the oxygen is more similar to a double charged peroxide anion than to O_2^- (1.34 Å) or the neutral O_2 (1.24 Å). The absence of magnetic moment for all the molecular adsorption states confirms the presence of adsorbed O_2^{2-}-like species.

The local charging–decharging of V5- and V6-like adsorbed structures was recently associated to the deviations from ordinary diffusion observed for oxygen on the TiO_2 surface.[9] Electronic charge transfers between O vacancies and adsorbed oxygen (and back) were suggested to enhance the diffusion rate along the rows. Our calculations show an effective charge transfer towards oxygen intermediates either adjacent or in close proximity to a vacancy; the reverse charge transfer probably requires the molecule to travel farther away from the vacancy than allowed by the size of our supercells.

The charge-transfer stabilization of O_2 molecules adsorbed on Ti_{5c} atoms adjacent to a vacancy requires these Ti_{5c} sites to be partially reduced before adsorption,[7] that is some delocalization of the density associated to the vacancy to the adjacent Ti_{5c} cations.[7] The density difference maps[16] shown in Figure 6

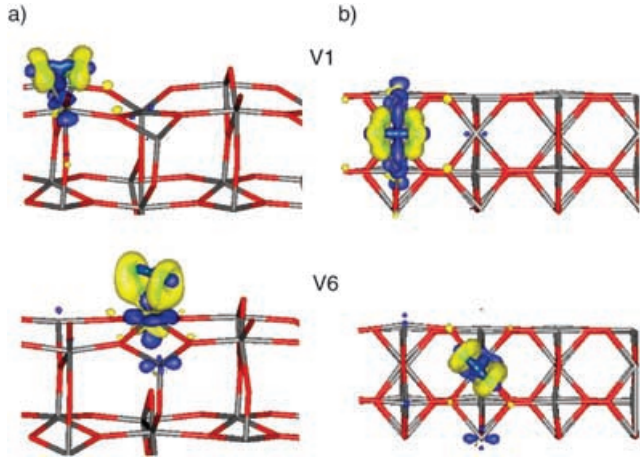

Figure 6. Density difference plots (contoured at 0.01 a.u.) for V1 and V6 adsorption structures: a) side view, b) top view. The flow of charge upon adsorption occurs from negative (contoured in blue) to positive regions (contoured in yellow).

confirm this point. In the V1 state, charge from the two Ti cations located in the vacancy is mostly transferred to the oxygen π^* orbitals, leading to a significant decrease of the charge along the O–O bond compared to an isolated O_2 molecule. In the V6 state, a similar amount of charge is transferred from the Ti_{5c} site to the O_2 π^* orbitals, with an analogous flow of charge out of the O–O bond. This suggests a similar oxidation state of adsorbed molecular oxygen at the vacancy or in the Ti_{5c} row. Plots similar to those of Figure 6 have been obtained also for the other oxygen-adsorption structures.

Simulated STM Images

Simulated STM images were obtained in the Tersoff–Hamann approximation[17] by integrating the local charge density of unoccupied states lying between ε_f and $\varepsilon_f + 1.3$ eV (where ε_f is the Fermi level). The resulting contour plots in a plane located $\approx$4 Å above the surface are shown in Figure 7. The STM for the perfect and defective clean surfaces are shown as reference: the higher density above the Ti_{5c} atoms is evident and is associated with the bright rows experimentally observed;[19] the charge spreads over the bridging oxygen rows only when a vacancy is created there. Structures V1 and O1, that is, when oxygen fills the vacancy, give rise to STM images rather similar to the clean surface; a higher density is actually present above the O–Ti_{5c} adatom in structure O1. When the vacancy is empty or only partially filled, like in structures V2, V5 and V6, the density is localized mostly above the adsorbed oxygen molecule, and to a lower extent above the two Ti^{3+} ions around the va-

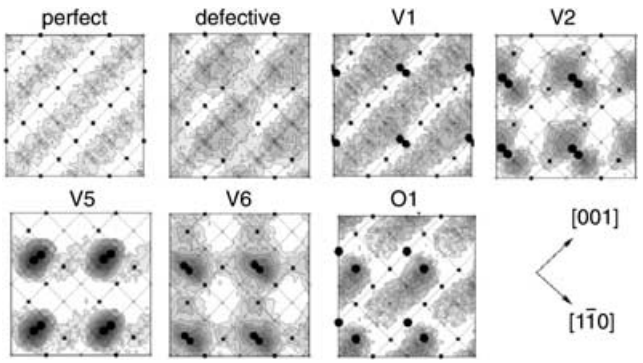

Figure 7. Simulated STM images calculated as integrated local density of states lying 1.3 eV above the Fermi level, contoured in a plane 4 Å above the surface. Darker areas correspond to higher density and thus to brighter features in experimental STM images. Small and large dots represent lattice and adsorbed oxygen, respectively.

cancy. In the experimental STM images[8] both the O_2 molecules adsorbed on top of Ti_{5c} atoms and the O–Ti_{5c} adatom appear as additional brighter features, in agreement with our results.

Conclusions

Herein, we have presented accurate first-principles calculations of the adsorption structures and reaction pathways of O_2 on the defective (partially reduced) rutile TiO2(110) surface. We have identified a number of distinct—both molecular and dissociated—configurations for adsorbed O_2, and determined the minimum-energy pathways for the transformations between these different states. Our results are in overall agreement with a variety of experimental findings, for example, in ref. [7] as well as with other recent theoretical studies.[14,15] A few differences between different theoretical results are likely to originate from differences in the computational setups, but still need to be understood in detail. Our calculated energetics and reaction barriers, together with the data in refs. [14] and [15], provide a framework for understanding recent STM observations of oxygen-assisted O-vacancy diffusion.[8] More specifically, after O_2 diffusion and dissociation at a vacancy, our calculations support an indirect pathway for the final steps of the vacancy migration process,[11] which does not require capture of a lattice oxygen, at variance with the direct mechanism originally proposed in ref. [8]. The key step in the overall process, as also recently found in ref. [15], turns out to be the O_2 dissociation step, with an energy barrier around 1.3 eV. The dissociated O adatoms could then diffuse away from the vacancy (Figure 3 e), but this path is hindered by higher energy barriers compared to the recombination–molecular diffusion steps (Figures 3 c1 and 3 b1) which eventually lead to vacancy migration. Moreover, we have found that a very effective charge transfer from the reduced surface takes place upon adsorption at a vacancy, where molecular oxygen is reduced to an O_2^{2-} ion. A large excess charge remains localized on the oxygen molecule in all its stable adsorption states, regardless of the distance from the vacancy, suggesting that the decharging process invoked in ref. [9] likely requires O_2 migration over several Ti_{5c} sites to be effective.

Computational Methods

Calculations have been performed by the Car–Parrinello[12] method, using the PBE exchange–correlation functional[21] and ultrasoft pseudo-potentials[22] including O 2s, 2p and Ti 3s, 3p, 3d, 4s shells. Plane-wave basis-set cutoffs for the smooth part of the wavefunctions and the augmented density were 25 and 200 Ry, respectively. *k*-Sampling was restricted to the Γ point. This approximation has been tested[11] and found reasonable for large supercells such as the one considered in this work (see below). Three-dimensional periodic-boundary conditions (PBC) were applied throughout, with a $\approx$10 Å vacuum layer along the *z* axis. The atoms in the bottom layer were always fixed to their bulk positions. The slab thickness is a very important and delicate issue when modeling the rutile(110) surface (for a recent discussion, see ref. [23]). After extensive testing,[11] in our case we found that four layers of Ti atoms (i.e., four O–Ti_2O_2–O trilayers) provided adequately converged results. *p*(2×2), *p*(1×3) and *c*(2×4) surface cells were considered (Figure 1). *p*(2×2) and *c*(2×4) cells have the same vacancy density (25%), but on the *c*(2×4) cell, the periodic images of the vacancies are staggered so that their nearest-neighbor distance is larger than the *p*(2×2) cell. This results in a less-repulsive vacancy–vacancy interaction, as shown by the calculated vacancy-formation energies (VFE) of 3.47, 3.76 and 4.06 eV for *c*(2×4), *p*(2×2) and *p*(1×3) cells, respectively. Therefore the effect of vacancy–vacancy interaction is weaker for the *c*(2×4) cell, and we focus mainly on the energies and barriers obtained on it. Geometry optimizations were carried out through damped MD until the largest component in the ionic forces was less than 0.025 eV $Å^{-1}$. Spin polarization was included when needed (bare defective surface).

After determining the optimized structure of relevant adsorption minima, the vacancy-migration barriers and minimum energy pathways (MEP) were calculated through the string-method Car–Parrinello (SMCP) approach.[13] In this approach, the end points of a reaction path are connected through a number of images (replicas) of the system, distributed along a "string". The perpendicular force acting on each replica is minimized by damped CP dynamics, while at the same time the geometrical constraints acting along the reaction path ensure that replicas are kept evenly spaced along the string. Because of the large size of our system, the number of replicas used in a SM minimization was usually set to six. We checked that no significant differences were present among the MEPs obtained on the *p*(2×2) cell using 6 and 10 replicas, respectively. Moreover, in several cases where the initial SM procedure indicated the presence of a stable intermediate between the end points, two separate SM optimizations were carried out, leading from the initial state to the intermediate and from this to the final state, and the two MEPs were matched at the intermediate state. Thus the overall MEP in these cases was actually represented by 11 replicas, with higher resolution and accuracy. Further details on the string method, its implementation and performance can be found in ref. [13], as well as in ref. [24], where this method has been recently applied to study reactions on silicon surfaces.

Acknowledgements

The calculations were performed on the Lemieux supercomputer at the Pittsburgh Supercomputing Center and on the IBM SP3 at the Princeton Institute for the Science and Technology of Materi-

als. This work was partially supported by the National Science Foundation under Grant No. CHE-0121432.

Keywords: density functional calculations · oxygen adsorption · surface chemistry · titanium oxide · vacancy diffusion

[1] U. Diebold, *Surf. Sci. Rep.* **2002**, *293*, 1.
[2] A. Linsebigler, G. Lu, J. T. Yates, *Chem. Rev.* **1995**, *95*, 735.
[3] M. R. Hoffmann, S. T. Martin, W. Choi, D. W. Bahnemann, *Chem. Rev.* **1995**, *95*, 69.
[4] C. L. Perkins, M. A. Henderson, *J. Phys. Chem. B* **2001**, *105*, 3856.
[5] A. Heller, *Acc. Chem. Res.* **1995**, *28*, 503.
[6] M. A. Henderson, W. S. Epling, C. H. F. Peden, C. L. Perkins, *J. Phys. Chem. B* **2003**, *107*, 534.
[7] M. A. Henderson, W. S. Epling, C. L. Perkins, C. H. F. Peden, U. Diebold, *J. Phys. Chem. B* **1999**, *103*, 5328.
[8] R. Schaub, E. Wahlstrom, A. Ronnau, E. Laegsgaard, I. Stensgaard, F. Besenbacher, *Science* **2003**, *299*, 277.
[9] E. Wahlstrom, E. K. Vestergaard, R. Schaub, A. Ronnau, M. Vestergaard, E. Laegsgaard, I. Stensgaard, F. Besenbacher, *Science* **2004**, *303*, 511.
[10] W. S. Epling, C. H. F. Peden, M. A. Henderson, U. Diebold, *Surf. Sci.* **1998**, *412-413*, 333.
[11] X. Wu, A. Selloni, M. Lazzeri, S. K. Nayak, *Phys. Rev. B* **2003**, *68*, 241 402.
[12] R. Car, M. Parrinello, *Phys. Rev. Lett.* **1985**, *55*, 2471.
[13] Y. Kanai, A. Tilocca, A. Selloni, R. Car, *J. Chem. Phys.* **2004**, *121*, 3359.
[14] M. D. Rasmussen, L. M. Molina, B. Hammer, *J. Chem. Phys.* **2004**, *120*, 988.
[15] Y. Wang, D. Pillay, G. S. Hwang, *Phys. Rev. B* **2004**, *70*, 193 410.
[16] Density difference maps were calculated as $\rho_{slab+O_2}(\vec{r})-\rho_{slab}(\vec{r})-\rho_{O_2}(\vec{r})$, ρ_{slab+O_2}, ρ_{slab} and ρ_{O_2} are the charge densities of the interacting system, the bare slab and the isolated O_2 molecule, respectively, with the latter two terms fixed at the geometry of the interacting system.
[17] J. Tersoff, D. Hamann, *Phys. Rev. Lett.* **1983**, *50*, 1998.
[18] The binding energy of an oxygen adatom was calculated as $E_{perf}+E_O-E_{O1}$, where E_{perf}, E_O and E_{O1} are the energies of the perfect surface, of an oxygen atom and of O1 adsorption state, respectively.
[19] U. Diebold, J. Anderson, K.-O. Ng, D. Vanderbilt, *Phys. Rev. Lett.* **1996**, *77*, 1322.
[20] Experimentally, defect states due to oxygen vacancies are $\approx$0.8 eV below the conduction-band edge. The incorrect energy position of calculated vacancy states is a known shortcoming of DFT, which does not well describe the localization of these states.
[21] J. P. Perdew, K. Burke, M. Ernzerhof, *Phys. Rev. Lett.* **1996**, *77*, 3865.
[22] D. Vanderbilt, *Phys. Rev. B* **1990**, *41*, 7892.
[23] L. A. Harris, A. A. Quong, *Phys. Rev. Lett.* **2004**, *93*, 086 105.
[24] N. Takeuchi, Y. Kanai, A Selloni, *J. Am. Chem. Soc.* **2004**, *126*, 15 890.

Received: November 28, 2004
Revised: February 21, 2005
Published online on August 4, 2005

